Supplemental Information

Structural Studies of *Methylosinus trichosporium* OB3b Soluble Methane Monooxygenase Hydroxylase and Regulatory Component Complex Reveal a Transient Substrate Tunnel

Jason C. Jones,[†,¶] Rahul Banerjee,[†,¶] Ke Shi,[†]

Hideki Aihara,[†] and John D. Lipscomb[†,¶,*]

[†] Department of Biochemistry, Molecular Biology, and Biophysics, and [¶]Center for Metals in Biocatalysis University of Minnesota, Minneapolis, Minnesota 55455, United States

Table of Contents

Analysis of Stopped-Flow Data. For a linear series of first order or pseudo-first order reactions, the time course can be fit by summing exponential expressions where the number of exponentials is equal to the number of steps, *n* (Eq. 1). If the steps are irreversible, then the reciprocal relaxation times (1/τ) give the rate constants for individual steps, although it is not possible to assign a specific reciprocal relaxation time to the rate constant for a specific step without additional information. When the steps are reversible, the reciprocal relaxation times become coupled, so that they do not correlate with a specific rate constant. In some cases, the rate constants can be determined from the ligand concentration dependence of the reciprocal relaxation times.[1]

$$Abs_t = \left(\sum_{i=1}^{n} Amp_i\, e^{-\frac{t}{\tau i}}\right) + Abs_{inf} \qquad \text{(Eq. 1)}$$

The kinetic data were fit to Eq. 1 using the nonlinear regression function of the Applied Photophysics ProData Viewer program. In this equation, Abs_t is the observed absorbance at time t, Amp_i is the observed amplitude for exponential phase *i*, τ_i is the relaxation time for phase *i*, and Abs_{inf} is the final absorbance at the end of the reaction. Fitting statistics were reported by the fitting program, and each reaction was repeated multiple times to determine the average fitting parameters and errors.

For a single step reaction (Eq. 2) only one exponential phase is observed under pseudo-first order conditions in ligand, allowing Eq. 3 to be used to determine the forward (k_r) and reverse (k_r) rate constants as well as the K_D from their ratio.

$$\text{E + ligand} \underset{k_r}{\overset{k_f}{\rightleftarrows}} \text{E·ligand} \qquad \text{(Eq. 2)}$$

$$\frac{1}{\tau_{obs}} = k_f[\text{ligand}] + k_r \qquad \text{(Eq. 3)}$$

For a two-step reaction where the first step is fast, reversible ligand binding (Eq. 4), only one exponential phase may be observed. A plot of $1/\tau_{obs}$ versus the concentration of the binding ligand will be hyperbolic if the rate constant k_{r1} is at least 3 fold greater than k_{f2} (Eq. 5).[2] The K_{D1} for the first step, k_{f2}, and k_{r2} are given by a non-linear regression fit to the hyperbolic plot.

$$\text{E + ligand} \underset{k_{r1}}{\overset{k_{f1}}{\rightleftarrows}} \text{E·ligand} \underset{k_{r2}}{\overset{k_{f2}}{\rightleftarrows}} \text{E-ligand'} \qquad \text{(Eq. 4)}$$

$$\frac{1}{\tau_{obs}} = \frac{k_{f2}[\text{ligand}]}{\left(\frac{k_{r1}}{k_{f1}}\right)+[\text{ligand}]} + k_{r2} \qquad \text{(Eq. 5)}$$

Table S1. MMOB Variant Primers

MMOB Mutant	Mutagenesis Forward Primer 5'-3'	Mutagenesis Reverse Primer 5'-3'
V41(WT)	GTGGTTCTGGTGCTGATGAAGAG	GGCGTTGGACTCGTGGAC
V41F	GTGGTTCTGTTCCTGATGAAGAG	GGCGTTGGACTCGTGGAC
V41R	GTGGTTCTGCGTCTGATGAAGAG	GGCGTTGGACTCGTGGAC
V41E	GTGGTTCTGGAGCTGATGAAGAG	GGCGTTGGACTCGTGGAC
V39F	AACGCCGTGTTTCTGGTGCT	GGACTCGTGGACGACCTG
V39R	AACGCCGTGCGTCTGGTGCT	GGACTCGTGGACGACCTG

Table S2. Data Collection and Refinement Statistics

	sMMOH^{ox}	sMMOH^{red}	sMMOH^{ox}:MMOB Form 1	sMMOH^{ox}:MMOB Form 2	sMMOH^{red}:MMOB
Data collection					
PDB Code	6VK6	6VK7	6VK5	6VK8	6VK4
Resolution range (Å)	63.8-1.52 (1.57 - 1.52)	49.1-2.12 (2.20 - 2.12)	73.5-1.86 (1.93 - 1.86)	86.0-2.03 (2.10 - 2.03)	52.6-2.35 (2.43 - 2.35)
Space group	$C222_1$	$C222_1$	$P2_12_12_1$	$P2_12_12_1$	$P2_12_12_1$
Unit cell (Å)	63.07 292.63 141.79	62.46 290.45 139.2	102.62 105.46 299.42	101.87 105.35 297.72	102.86 105.21 300.88
Total reflections	628962 (60913)	363811 (33807)	1365173 (131835)	858293 (87118)	576343 (57098)
Unique reflections	197515 (19628)	71995 (7050)	271076 (26707)	203936 (19538)	133740 (11725)
Multiplicity	3.2 (3.1)	5.1 (4.8)	5.0 (4.9)	4.2 (4.3)	4.3 (4.3)
Completeness (%)	98.25 (98.37)	99.37 (98.84)	99.65 (99.26)	97.85 (95.35)	96.27 (86.80)
I/σI	11.58 (1.14)	6.69 (1.08)	8.21 (0.97)	8.09 (0.95)	5.71 (0.65)
R-merge	0.06956 (1.023)	0.1599 (1.366)	0.131 (1.511)	0.137 (2.025)	0.1447 (2.263)
R-meas	0.08342 (1.234)	0.1784 (1.534)	0.1463 (1.691)	0.152 (2.316)	0.1641 (2.574)
R-pim	0.04492 (0.6755)	0.07791 (0.6875)	0.06397 (0.7467)	0.096 (1.105)	0.07547 (1.195)
$CC_{1/2}$	0.998 (0.532)	0.994 (0.442)	0.996 (0.39)	0.992 (0.387)	0.993 (0.392)
Refinement					
Reflections	197477 (19613)	71994 (7048)	270965 (26698)	202459 (19516)	131580 (11717)
# used for R-free	9858 (1002)	3609 (398)	13530 (1336)	10347 (1019)	6689 (597)
R-work	0.1392 (0.3111)	0.1600 (0.2659)	0.1721 (0.2965)	0.1664 (0.3154)	0.2088 (0.3991)
R-free	0.1585 (0.3048)	0.2027 (0.3213)	0.1933 (0.3108)	0.2073 (0.3445)	0.2379 (0.4275)
# of non-H atoms	10110	9437	21007	20999	19851
Macromolecules	8814	8697	19498	19498	19475
Ligands	201	2	123	116	78
Solvent	1095	738	1386	1385	298
RMS deviation					
Bond lengths (Å)	0.011	0.010	0.005	0.007	0.003
Bond angles (º)	1.03	1.00	0.86	0.85	0.57
Ramachandran plot					
Favored (%)	97.18	97.37	96.96	97.13	96.51
Allowed (%)	2.82	2.63	2.95	2.87	3.37
Outliers (%)	0.00	0.00	0.08	0.00	0.12
Average B-factor	22.14	36.94	28.46	36.59	63.63
Macromolecules	20.29	36.44	28.28	36.15	63.57
Ligands	46.47	34.96	34.43	51.86	102.92
Solvent	32.52	42.89	30.50	41.52	57.03

Table S3. Interatomic Distances for sMMOH

Ligand-Fe	sMMOH^{ox} (6VK6)	sMMOH^{red} (6VK7)
Resolution	1.52 Å	2.12 Å
Fe1-Fe2	3.1	3.3
Fe1-E114 OE1	2.0	2.1
Fe1-E144 OE1	2.1	2.3
Fe1-E243 OE2	3.9	2.2
Fe1-H147 ND1	2.2	2.2
Fe1-HOH 1	2.2	2.4
Fe1-HO(H) 2[a]	2.1	2.5
Fe1-EDO O2[a]	2.1	N/A
Fe2-E209 OE2	1.9	2.0
Fe2-E243 OE2	3.4	2.4
Fe2-E243 OE1	2.2	2.2
Fe2-E144 OE2	2.2	2.2
Fe2-H246 ND1	2.2	2.2
Fe2-EDO O2[a]	2.4	N/A
Fe2-HO(H) 2[a]	1.9	2.3

[a]Bridging

Rare Types of Helices within sMMOH. Close inspection of the *Mt* sMMOH and *Mt* sMMOH:MMOB crystal structures obtained in this study provided detailed information about the helical composition of the sMMOH α-subunit as summarized in Table S4. Principal helices A, D, E, H, and a helix formed by residues W379 to L393 contain π-helices, where the backbone carbonyl of residue i hydrogen bonds to the backbone NH moiety of the i+5 residue in at least 2 consecutive residues (Figure S1). Two of these π-helices (in Helices E and H) have been described previously in limited detail.[3-5] The helix composed of residues W379 to L393 is involved in making crystal contacts, and the backbone carbonyl group of residue W379 is engaged in a rare trifurcated acceptor hydrogen bond, which initiates the π-helix. Because this π-helix is involved in crystal contacts, we assume it an artifact of protein crystallization, and therefore not functionally important. When the complex with MMOB forms, Helix E residues N214 and P215 as well as Helix H residues G314 and G315 form additional π-helices (Figure S1). The π-helix in Helix D, composed of residues K185 and R186, becomes a coiled region as a result of large exogenous molecules present in the active site in Forms 1 and 2 crystals. It is interesting to note that many of the residues that stabilize the α-helices throughout the α-subunit also form hydrogen bonds to the i + 3 residue (a 3_{10} helix, Table S4). Typically, 3_{10} helices are located at the ends of α-helices, but this is not universally the case in sMMOH. The partial 3_{10} helix character causes the α-helices to be tightly wound, further highlighting the flexibility of the interspersed π-helical segments.

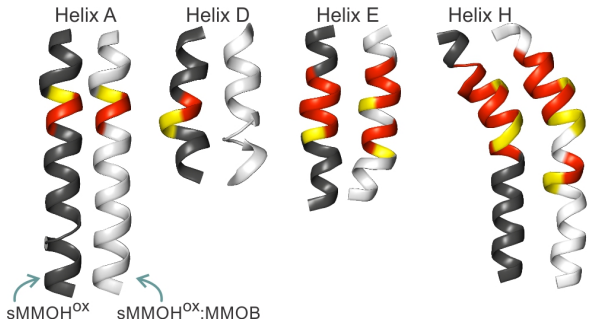

Figure S1. The π-helices of *Mt* sMMOH^{ox} (6VK6) and *Mt* sMMOH^{ox}:MMOB (6VK5) crystal structures. sMMOH and sMMOH:MMOB Helices A, D, E, and H are represented as grey and white cartoons, respectively. The π-helices are colored red and sections of the protein that do not form intra-main chain hydrogen bonds are colored yellow.

Table S4. Assignment of Secondary Structures

1.52 Å sMMOH^{ox} protomer 1

Residues	i	i + 3	i + 4	I + 5	distances
25-35	P25				
Helix 1	Q26		K30		2.4
	E27				
	V28	W31			2.1
	H29	L32			2
	K30				
	W31	S34			2.4
	L32	F35			2
64-89	A64		A68		2.3
Helix A	K65	A68	R69		2.9, 2.2
	E66	R69	M70		2.9, 2.1
	Y67	M70	E71		2.9,2.3
	A68	E71	A72		2.9,2.1
	R69		A73		2.5
	M70	S73	K74		2.8, 2.6
	E71	K74	D75		2.7, 2.2
	A72	D75	E76		2.7, 2.2
	A73		R77		2.7
	K74	R77	Q78		2.8, 2.3
	D75	Q78	F79		2.9, 2.0
	E76		G80		2.2
	R77		T81		2.3
	Q78	T81	L82		2.9, 2.2
	F79		L83		2.1
	G80		D84	G85	2.1, 2.6
	T81		G85	L86	2.8, 2.0
	L82			T87	2.8
	L83				
	D84		R88		2.3
	G85	R88	L89		2.8, 2.4
	L86	L89	G90		2.6, 2.7
	T87	G90			2.2
97-126	P97	G100	E101		2.9,2.2
Helix B	R98	E101	T102		2.9, 2.2
	W99		M103		2.2
	G100				
	E101	K104			2.3
	T102	V105	I106		2.4, 2.0
	M103		S107		2.3
	K104		N108		2.6
	V105		F109		1.9
	I106		L110		2.1
	S107		E111		2.2
	N108		V112		2.7
	F109	V112			2.5
	L110	G113	E114		2.5, 2.1
	E111	E114	Y115		2.9, 2.0
	V112		N116		2
	G113		A117		2.2
	E114	A117	I118		2.8, 2.7
	Y115	I118			2.4
	N116	A119	A120		2.7, 2.1
	A117		S121		2.1
	I118	S121	A122		2.9, 2.2
	A119	A122	M123		2.7, 2.2
	A120	M123	L124		2.7, 2.2
	S121		W125		2
	A122		D126		2.2
	M123		S127		2.3
	L124	S127			2.4
131-161	A131		N135		2.1
Helix C	E132		G136		2.2
	Q133	G136	Y137		2.7, 2.3
	K134	Y137	L138		2.8, 2.1
	N135		A139		2.2
	G136	A139	Q140		2.9, 2.6
	Y137	Q140	V141		2.6, 2.1
	L138	V141	L142		2.7, 2.2
	A139	L142	D143		2.8, 2.1
	Q140	D143	E144		2.7, 2.0
	V141	E144	I145		2.8, 2.5
	L142	I145	R146		2.7, 2.3
	D143		H147		2.1
	E144		T148		2.1
	I145	T148	H149		2.7, 2.3
	R146	H149	Q150		2.7, 2.2
	H147		C151		2.1
	T148		A152		2.1
	H149		F153		2.1
	Q150		I154		2.3
	C151	I154	N155		2.7,2.5
	A152	N155	H156		2.7,2.0
	F153		Y157		1.9
	I154	Y157	Y158		2.8,2.1
	N155		S159		2
	H156		K160		2.5
	Y157	K160	H161		2.4,2.4
	Y158	H161			2.5
171-177	A171		A175		2.1
	R172				
	R173	A176			2.4
	T174	I177			2.3
	R175	G178			2.5

2.12 Å sMMOH^{red} protomer 1

Residues	i	i + 3	i + 4	I + 5	distances
25-35	P25	V28	H29		3.2,2.9
Helix 1	Q26		K30		3.3
	E27				
	V28	W31			2.9
	H29	L32			3
	K30				
	W31	S34			3.2
	L32	F35			2.8
64-89	A64		A68		3.1
Helix A	K65		R69		3.1
	E66		M70		3
	Y67		E71		3.1
	A68	E71	A72		3.2, 2.8
	R69		A73		3.2
	M70		K74		3.5
	E71	K74	D75		3.0, 2.9
	A72		E76		3.1
	A73		R77		3.5
	K74	R77	Q78		3.3, 3.1
	D75	Q78	F79		3.1, 2.8
	E76		G80		3
	R77	G80	T81		3.3, 3.1
	Q78		L82		3.1
	F79		L83		3
	G80		D84	G85	2.9, 3.4
	T81		G85	L86	3.4, 2.8
	L82				
	L83				
	D84		R88		3.2
	G85	R88	L89		3.2, 3.1
97-101	P97		E101		2.9
Helix B	R98				
	W99				
	G100				
	E101				
102-127	M103		S107		3
Helix B	K104				
	V105	N108	F109		3.4,2.8
	I106		L110		3
	S107		E111		2.8
	N108		V112		3.2
	F109	V112	G113		3.3, 3.6
	L110	G113	E114		3.0, 2.9
	E111	E115	Y115		3.1, 2.8
	V112		N116		2.9
	G113		A117		3.1
	E114	A117	I118		3.1, 3.3
	Y115	I118			3
	N116	A119	A120		3.1, 2.9
	A117		S121		3
	I118		A122		3
	A119		M123		2.9
	A120		L124		3
	S121		W125		2.9
	A122		D126		2.9
	M123		S127		3
	L124	S127			2.9
131-161	A131		N135		2.9
Helix C	E132		G136		3
	Q133	G136	Y137		3.2, 3.2
	K134		L138		2.9
	N135		A139		2.9
	G136		Q140		3.2
	Y137		V141		2.8
	L138	V141	L142		2.9, 3.0
	A139	L142	D143		3.3, 3.0
	Q140		E144		2.9
	V141		I145		3.3
	L142	I145	R146		3, 3
	D143	R146	H147		3, 2.8
	E144		T148		3
	I145		H149		3.1
	R146	H149	Q150		3.2, 2.8
	H147		C151		2.9
	T148		A152		3
	H149		F153		2.9
	Q150		I154		3
	C151	I154	N155		3.2, 3.4
	A152	N155	H156		3.2, 2.7
	F153		Y157		2.8
	I154	Y157	Y158		3.1, 2.9
	N155		S159		2.9
	H156		K160		3.3
	Y157	K160	H161		2.9, 3.0
	Y158	H161			3.2
174-177	T174	I177			3.2

1.86 Å sMMOH^{ox}:MMOB Form 1, protomer 1

Residues	i	i + 3	i + 4	I + 5	distances
25-35	P25	V28	H29		2.7, 2.1
Helix 1	Q26		K30		2.5
	E27				
	V28	W31			2.1
	H29	L32			2.2
64-89	A64		A68		3.1
Helix A	K65		R69		3.4, 3.1
	E66		M70		3.1
	Y67	M70	E71		3.2
	A68	E71	A72		2.9, 2.3
	R69		A73		2.3
	M70	A73	K74		2.9, 2.3
	E71	K74	D75		2.8, 2.1
	A72		E76		2.1
	A73		R77		2.7
	K74		Q78		2.3
	D75	Q78	F79		2.8, 1.9
	E76		G80		2.2
	R77		T81		2.2
	Q78		L82		2.3
	F79		L83		2
	G80		D84	G85	2.2, 2.7
	T81			L86	2
	L82			T87	2.8
	L83				
	D84	T87	R88		2.7, 2.2
	G85	R88	L89		2.8, 2.3
	L86	L89			2.7
97-127	P97		E101		2.2
Helix B	R98		T102		2.2
	W99	T102	M103		2.7, 2.2
	G100				
	E101	K104			2.6
	T102	V105	I106		2.4, 2.1
	M103		S107		2.2
	K104		N108		2.6
	V105		F109		2
	I106		L110		2.1
	S107		E111		2.1
	N108		V112		2.7
	F109	V112	G113		2.5, 2.5
	L110	G113	E114		2.6, 1.9
	E111	E114	Y115		2.9, 2.1
	V112		N116		2
	G113		A117		2
	E114	A117	I118		2.6, 2.5
	Y115	I118			2.4
	N116	A119	A120		2.5, 2.0
	A117		S121		2
	I118		A122		2.2
	A119	A122	M123		2.5, 2.3
	A120	M123	L124		2.5, 2.2
	S121		W125		2
	A122		D126		1.9
	M123		S127		2.1
	L124	S127			2.8
131-161	A131	K134	N135		2.8, 2.0
Helix C	E132		G136		2.2
	Q133		Y137		2
	K134	Y137	L138		2.9, 2.3
	N135	L138	A139		2.7, 2.5
	G136		Q140		2.4
	Y137		V141		2
	L138		L142		2.1
	A139	L142	D143		2.9, 2.1
	Q140	D143	E144		2.7, 2.1
	V141	E144	I145		2.8, 2.5
	L142	I145	R146		2.6, 2.1
	D143		H147		2
	E144		T148		2.2
	I145	T148	H149		2.6, 2.3
	R146	H149	Q150		2.6, 2.1
	H147		C151		2.1
	T148		A152		2.1
	H149		F153		2.1
	Q150	F153	I154		2.5, 2.3
	C151	I154	N155		2.7, 2.6
	A152	N155	H156		2.8, 2.0
	F153		Y157		1.9
	I154	Y157	Y158		2.8, 2.0
	N155		S159		2
	H156	S159	K160		2.7, 2.4
	Y157	K160	H161		2.4, 2.3
	Y158	H161			2.6
171-177	A171		R175		2
	R172				
	R173	A176			2.4
	T174	I177			2.3
	R175				

2.5 Å sMMOH^{red}:MMOB protomer 1

Residues	i	i + 3	i + 4	I + 5	distances
25-35	P25	V28	H29		3.0, 2.9
Helix 1	Q26		K30		3.4
	E27				
	V28	W31			3
	H29	L32			3.1
64-89	A64	Y67	A68		3.2, 3.1
Helix A	K65		R69		3.1
	E66		M70		3
	Y67		E71		3.2
	A68		A72		2.9
	R69		A73		3.2
	M70	A73	K74		3.0, 3.0
	E71	K74	D75		3.2, 2.8
	A72		E76		3
	A73		R77		3.5
	K74	R77	Q78		3.4, 3.0
	D75		F79		2.8
	E76		G80		2.8
	R77		T81		3
	Q78	T81	L82		3.4, 3.1
	F79		L83		2.8
	G80		D84	G85	3.2, 3.3
	T81			L86	2.8
	L82			T87	3.3
	L83				
	D84		R88		3
	G85	R88	L89		3.2, 3.1
97-127	P97		E101		3
Helix B	R98		T102		3.1
	W99		M103		3
	G100	M103			3.3
	E101	K104			2.9
	T102	V105	I106		3.2, 2.9
	M103		S107		3.1
	K104		N108		3.5
	V105		F109		2.9
	I106		L110		2.9
	S107		E111		2.9
	N108		V112		3.2
	F109	V112	G113		3.3, 3.2
	L110	G113	E114		3.1, 2.7
	E111		Y115		2.8
	V112		N116		2.9
	G113		A117		2.9
	E114		I118		3.1
	Y115	I118			3.1
	N116	A119	A120		3.1, 2.9
	A117		S121		2.9
	I118		A122		3.1
	A119	A122	M123		3.0, 3.0
	A120	M123	L124		3.1, 3.1
	S121	L124	W125		3.1, 2.7
	A122		D126		2.8
	M123		S127		2.8
131-161	A131		N135		3
Helix C	E132		G136		2.8
	Q133		Y137		2.8
	K134		L138		3.1
	N135		A139		3.2
	G136		Q140		3.1
	Y137		V141		2.9
	L138		L142		2.9
	A139		D143		2.9
	Q140		E144		3
	V141	E144	I145		3.4, 3.3
	L142	I145	R146		3.1, 3.0
	D143		H147		2.8
	E144		T148		3
	I145		H149		3.2
	R146	H149	Q150		3.2, 2.9
	H147		C151		3
	T148		A152		2.8
	H149		F153		2.8
	Q150		I154		3
	C151		N155		3.6
	A152		H156		2.9
	F153		Y157		2.7
	I154		Y158		2.8
	N155		S159		2.9
	H156	S159	K160		3.3, 3.4
	Y157	K160	H161		3.0, 3.1
	Y158	H161			3.4
174-177	T174	I177			3.4

179-193	P179	K182			2.6
Helix D	L180	G183	M184		2.9, 2.5
	W181	M184	K185		2.6, 2.3
	K182	K185	R186		2.7, 2.6
	G183	R186	V187		2.6, 2.5
	M184	V187	F188		2.9, 2.1
	K185		A189	D190	2.3, 1.9
	R186			G191	2.1
	V187				
	F188				
	A189	F192			2.4
	D190	I193			2.3
197-227	A197	S201			2
Helix E	V198		V202		2.2
	E199	V202	N203		2.7, 2.2
	C200	N203	L204		2.8, 2.0
	S201		Q205	L206	2.1, 24
	V202			V207	2
	N203			G208	2.1
	L204			E209	2
	Q205			A210	2.3
	L206				
	V207		C211	F212	2.0, 2.7
	G208		F212	T213	2.5, 1.9
	E209			N214	2.1
	A210				
	C211				
	F212		L216		2
	T213		I217		2
	N214				
	P215	V218	A219		2.8, 2.0
	L216	A219	V220		2.7, 1.9
	I217		T221		2.6
	V218	T221	E222		2.4, 25
	A219	E222	W223		2.3, 2.1
	V220		A224		2
	T221		S225		2.1
	E222		A226		2.2
	W223		N227		2.5
	A224	N227			2.3
230-258	E230		T234		2.7
Helix F	I231	T234	V235		2.7, 2.5
	T232	V235	F236		2.7, 1.9
	P233		L237		2.1
	T234				
	V235	S238	V239		2.3, 2.1
	F236		E240		2.1
	L237				
	S238	T241			2.4
	V239	D242			2.2
	E240	E243			2.3
	T241				
	D242	R245			2.8
	E243	H246	M247		2.3, 2.2
	L244		A248		2.1
	R245		N249		2.3
	H246	N249	G250		2.6, 2.3
	M247	G250	Y251		2.6, 2.2
	A248	Y251	Q252		2.8, 2.0
	N249		T253		2.1
	G250	T253	V254		2.6, 2.5
	Y251	V254	V255		2.6, 2.1
	Q252		S256		2
	T253	S256	I257		2.7, 2.7
	V254	I257	A258		2.5, 2.9
	V255	A258			2.4

179-193	P179	K182			3.3
Helix D	L180		M184		3.5
	W181	M184	K185		3, 3
	K182	K185	R186		3.1, 3.3
	G183	R186	V187		3.3, 3.4
	M184		F188		2.8
	K185		A189	D190	3.0, 2.6
	R186			G191	2.8
	V187				
	F188				
	A189	F192			3.1
	D190	I193			3.1
197-227	A197		S201		2.7
Helix E	V198		V202		3
	E199		N203		3.1
	C200		L204		2.8
	S201		Q205	L206	2.6, 3.2
	V202			V207	2.9
	N203			G208	2.9
	L204			E209	2.9
	Q205			A210	2.8
	L206		A210		2.8
	V207		C211	F212	2.9, 2.9
	G208			T213	3.2
	E209		T213		3.4
	A210				
	C211				
	F212		L216		2.9
	T213		I217		2.9
	N214	I217	V218		3.2, 3.0
	P215		A219		3
	L216		V220		2.7
	I217		T221		2.9
	V218		E222		2.9
	A219	E222	W223		3.2, 2.7
	V220		A224		2.9
	T221		S225		3
	E222		A226		3.1
	W223		N227		3.3
	A224	N227			3
230-257	E230				
Helix F	I231	T234	V235		3.2, 3.3
	T232	V235	F236		3.3, 2.9
	P233		L237		3.1
	T234				
	V235	S238	V239		2.8, 2,9
	F236		E240		3
	L237				
	S238	T241			3.2
	V239	D242	E243		3.2, 3.0
	E240		L244		3.2
	T241				
	D242	R245			3
	E243	H246	M247		3.1, 3.2
	L244		A248		3.5
	R245		N249		3.1
	H246		G250		3
	M247		Y251		3
	A248		Q252		3.1
	N249	Q252	T253		3.1, 2.9
	G250		V254		3.4
	Y251	V254	V255		3.2, 3.0
	Q252		S256		2.8
	T253		I257		3.4
	V254	I257			3.4

179-187	P179	K182			2.6
Helix D	L180				
	W181	M184	K185		2.4, 2.5
	K182	K185			2.6
	G183	R186	V187		2.4, 2.2
	M184				
	K185				
	R186				
	V187				
	F188				
	A189				
190-193	D190	I193			2.8
197-227	A197	C200			2.5
Helix E	V198	S201			2.1
	E199	V202	N203		
	C200		L204	Q205	2.5, 2.5
	S201			L206	2.2
	V202			V207	2.3
	N203			G208	2
	L204			E209	2
	Q205		E209	A110	2.9, 2.1
	L206				
	V207		C211	F212	2.0, 2.5
	G208		F212	T213	2.3, 2.4
	E209				
	A210				
	C211				
	F212		L216		2.3
	T213		I217		2
	N214		V218	A219	2.2, 2.0
	P215			V220	2.7
	L216				
	I217				
	V218	T221			2.2
	A219	E222			2.3
	V220	W223	A224		2.5, 2.1
	T221		S225		2.2
	E222		A226		2.2
	W223	A226	N227		2.9, 2.2
	A224	N227			2.4
230-259	E230		T234		2.7
Helix F	I231	T234	V235		2.5, 2.5
	T232	V235	F236		2.6, 2.0
	P233		L237		2.3
	T234				
	V235	S238	V289		2.3, 2.0
	F236		E240		2.3
	L237				
	S238	T241			2.5
	V239	D242			2.3
	E240	E243			2
	T241				
	D242	R245			2.8
	E243	H246	M247		2.5, 2.1
	L244		A248		2.4
	R245		N249		2.1
	H246	N249	G250		2.8, 2.2
	M247	G250	Y251		2.7, 2.0
	A248		Q252		2.4
	N249	Q252	T253		2.7, 2.7
	G250	T253	V254		2.6, 2.1
	Y251	V254	V255		2.6, 2.1
	Q252	S256			2.5
	T253	S256	I257		2.7, 2.2
	V254	I257	A258		2.8, 2.1
	V255	A258	N259		2.8, 2.3
	S256	N259			2.6

179-187	P179	K182			3
Helix D	L180		M184		3.5
	W181	M184	K185		3.1, 3.2
	K182	K185			3.2
	G183	R186	V187		3.1, 3.2.
	M184				
	K185				
	R186				
	V187				
	F188				
	A189				
190-193	D190	I193			3.3
197-227	A197	C200			3
Helix E	V198	S201			3.1
	E199	V202	N203		2.7, 3.1
	C200		L204	Q205	2.9, 3.1
	S201			L206	3.1
	V202			V207	2.9
	N203			G208	3
	L204			E209	2.7
	Q205		E209	A210	3.2, 2.8
	L206				
	V207		C211	F212	3.4, 3.4
	G208		F212	T213	3.1, 3.1
	E209				
	A210				
	C211				
	F212		L216		3.2
	T213		I217		2.8
	N214		V218	A219	2.9, 3.0
	P215				
	L216				
	I217				
	V218	T221			3
	A219	E222			3.2
	V220	W223	A224		3.1, 2.9
	T221		S225		3
	E222		A226		2.9
	W223		N227		3.2
	A224	N227			3.1
230-259	E230				
Helix F	I231	T234	V235		3.2, 3.2
	T232	V235	F236		3.1, 2.6
	P233		L237		3.1
	T234				
	V235	S238	V239		3.0, 2.8
	F236		E240		3
	L237		T241		3.5
	S238	T241			3.4
	V239	D242			3.3
	E240	E243			2.8
	T241				
	D242	R245	H246		3.1, 3.5
	E243		M247		3.2
	L244		A248		3.5
	R245		N249		3
	H246	N249	G250		3.3, 3.1
	M247		Y251		3
	A248	Y251	Q252		3.3, 3.2
	N249	Q252			3.4
	G250	T253	V254		3.1, 3.0
	Y251		V255		3
	Q252		S256		3.4
	T253	S256	I257		3.0, 2.9
	V254		A258		3
	V255	A258	N259		3.1, 2.8

261-293	P261	A264	K265		2.9, 2.7
Helix G	A262	K265	F266		2.6, 2.3
	S263	F266	L267		2.5, 2.0
	A264				
	K265				
	F266	T269	D270		2.5, 2.3
	L267	D270	L271		2.8, 2.0
	N268		N272		2.1
	T269		N273		2.1
	D270		A274		2.1
	L271	A274	F275		2.8, 1.9
	N272		W276		2.1
	N273		T277		2.1
	A274	T277	Q278		2.9, 2.1
	F275	Q278	Q279		2.8, 2.2
	W276		K280		2.1
	T277	K280			2.8
	Q278	Y281	F282		2.7, 2.3
	Q279		T283		2.1
	K280				
	Y281		V285		2.2
	F282		L286		2.2
	T283				
	P284		Y288		2.4
	V285	Y288	L289		2.8, 2.1
	L286		F290		2.1
	G287		E291		2.1
	Y288		Y292		2.1

261-292	P261	A264	K265		3.3, 3.5
Helix G	A262		F266		3
	S263	F266	L267		3.4, 2.9
	A264				
	K265				
	F266	T269	D270		3.0, 3.1
	L267	D270	L271		3.2, 3.9
	N268		N272		3
	T269		N273		3.1
	D270		A274		2.9
	L271		F275		2.7
	N272		W276		3
	N273		T277		2.9
	A274		Q278		2.9
	F275		Q279		2.9
	W276		K280		2.9
	T277				
	Q278	Y281	F282		3.5, 2.9
	Q279		T283		3.1
	K280				
	Y281		V285		2.9
	F282		L286		3.3
	T283		G287		3.2
	P284		Y288		2.9
	V285		L289		2.9
	L286		F290		2.8
	G287		E291		3
	Y288		Y292		2.9

261-293	P261	K265			2.6
Helix G	A262				
	S263	F266			2.3
	A264	L267			2.3
	K265				
	F266		D270		2.3
	L267	D270	L271		2.9, 2.1
	N268		N272		2.2
	T269	N272	N273		2.9, 2.1
	D270		A274		2.1
	L271	A274	F275		2.8, 2.0
	N272		W276		2.1
	N273		T277		2.1
	A274		Q278		2.1
	F275		Q279		2
	W276		K280		2
	T277				
	Q278	Y281	F282		2.7, 2.1
	Q279		T283		2
	K280				
	Y281		V285		2.2
	F282		L286		2.2
	T283		G287		2.5
	P284		Y288		2.2
	V285		L289		2.2
	L286		F290		2
	G287		E291		2.2
	Y288		Y292		2.1

261-293	P261				
Helix G	A262				
	S263	F266			3.3
	A264	L267			3.2
	K265				
	F266		D270		3.2
	L267	D270	L271		3.3, 2.8
	N268		N272		3
	T269		N273		2.9
	D270		A274		2.9
	L271	A274	F275		3.2, 2.8
	N272		W276		3
	N273		T277		2.8
	A274		Q278		3
	F275		Q279		2.8
	W276		K280		2.8
	T277				
	Q278		F282		3
	Q279		T283		3.1
	K280				
	Y281		V285		3
	F282		L286		3
	T283		G287		3.3
	P284		Y288		3.1
	V285		L289		3
	L286		F290		3
	G287		E291		3.2
	Y288		Y292		2.9

301-322	W301	T304	W305		2.8, 1.9
Helix H	V302		N306		2.5
	K303	N306	R307		2.9, 2.4
	T304	R307	W308		2.7, 2.0
	W305		V309		2
	N306		Y310	E311	2.5, 2.2
	R307			D312	1.9
	W308			W313	2.3
	V309			G314	1.9
	Y310			G315	2.7
	E311		G315	I316	2.5, 2.4
	D312		I316	W317	2.9,2.1
	W313		W317	I318	2.9, 2.0
	G314				
	G315		G319		2.2
	I316	G319	R320		2.7, 2.5
	W317	R320			2.6
	I318		L321		2.1
	G319	G322			2.2

301-322	W301	T304	W305		3.0, 2.8
Helix H	V302		N306		2.9
	K303		R307		3
	T304		W308		3.2
	W305		V309	Y310	2.8, 3.4
	N306		Y310	E311	3.2, 3.0
	R307			D312	3
	W308			W313	2.9
	V309			G314	2.9
	Y310				
	E311		G115	I316	3.0, 3.5
	D312		I316	W317	2.9, 3.1
	W313			I318	2.9
	G314				
	G315		G319		3
	I316	G319	R320		3.1, 3.0
	W317	R320	L321		3.2, 3.1
	I318		G322		3.2
	G319	G322			3
	R320	K323			3.2
	L321	Y324			2.9

301-324	W301	T304	W305		2.5, 2.0
Helix H	V302		N306		2
	K303		R307		2.1
	T304		W308		2.2
	W305		V309	Y310	2.1, 2.4
	N306		Y310	E311	2.9,1.9
	R307			D312	2.3
	W308			W313	2.1
	V309			G314	2.2
	Y310				
	E311		G315		1.9
	D312	G315	I316		2.8, 1.9
	W313		W317	I318	2.2, 2.5
	G314			G319	1.9
	G315			R320	2.6
	I316				
	W317		L321		2.2
	I318		G322		2.4
	G319	G322			2.4
	R320	K323			2.3
	L321	Y324			2.1

301-323	W301		W305		2.8
Helix h	V302		N306		2.8
	K303		R307		2.8
	T304		W308		3.1
	W305		V309	Y310	2.8,3.2
	N306			E311	2.9
	R307			D312	3
	W308			W313	3
	V309			G314	2.9
	Y310				
	E311		G315		2.7
	D312		I316		2.7
	W313		W317	I318	3.0, 3.3
	G314			G319	2.5
	G315			R320	3.1
	I316				
	W317		L321		3.1
	I318		G322		3
	G319	G322			3.3
	R320	K323			3.6

332-335	L332	A335			2.7
	R333				
	D334				
	A335				
	K336				
	R337				
	D338				
	A339				
	Y340				
	W341				
342-356	A342		L346		2.2
	H343		A347		2.2
	H344		L348		2.5
	D345	L348	A349		2.6, 2.8
	L346	A349	A350		2.5, 2.0
	A347	A350	Y351		2.9, 2.0
	L348		A352		2.2
	A349	A352	M353		2.8, 2.3
	A350	M353			2.8
	Y351	W354			2.6
	A352				
	M353	L356			2.2

332-356	L332		K336		3.1
	R333	K336	R337		3.1, 3.3
	D334		D338		3.2
	A335		A339		3
	K336	A339			3.2
	R337	Y340			3.5
	D338	W341	A342		3.3, 2.8
	A339				
	Y340				
	W341	H344	D345		3.1, 3.0
	A342		L346		3
	H343		A347		2.9
	H344		L348		3.2
	D345	L348	A349		3.2, 3.5
	L346	A349	A350		2.9, 2.8
	A347		Y351		2.8
	L348		A352		2.9
	A349		M353		2.9
	A350				
	Y351	W354			3.4
	A352				
	M353	L356			3

331-356	S331	D334	A335		2.7,2.2
	L332	A335	K336		2.4, 2.0
	R333	K336	R337		2.8, 2.4
	D334		D338		2.5
	A335	D338	A339		2.4, 2.1
	K336	A339	Y340		2.7, 2.6
	R337	Y340	W341		2.6, 2.3
	D338		A342		2
	A339				
	Y340				
	W341	H344	D345		2.4, 2.3
	A342		L346		2
	H343		A347		2.2
	H344	A347	L348		2.8, 2.6
	D345	L348	A349		2.5, 2.7
	L346	A349	A350		2.5, 2.0
	A347		Y351		2
	L348		A352		2.1
	A349		M353		2.2
	A350	M353			2.8
	Y351	W354			2.7
	A352				
	M353	L356			2.2

332-355	L332	A335	K336		3.0, 2.8
	R333		R337		3.2
	D334		D338		3.1
	A335	D338	A339		3.1, 2.8
	K336		Y340		3.1
	R337		W341		3.2
	D338	W341	A342		3.5, 2.9
	A339				
	Y340				
	W341	H344	D345		3.1, 3.1
	A342	D345	L346		3.0, 2.8
	H343		A347		3
	H344		L348		3.3
	D345	L348	A349		3.0, 3.4
	L346	A349	A350		3.2, 2.8
	A347		Y351		2.9
	L348		A352		3.1
	A349		M353		2.9
	A350				
	Y351	W354			3.5
	A352				
	M353	L356			2.2

366-375	E366		A370		2.3
	E367	A370	W371		2.8, 2.3
	D368	W371	F372		2.5, 2.0
	Q369	F372	E373		2.9, 2.2
	A370		A374		2.2
	W371	A374	N375		2.8,2.3
	F372	N375	Y376		2.8, 2.0

366-375	E366		A370		3
	E367		W371		3
	D368		F372		2.8
	Q369		E373		2.9
	A370		A374		2.9
	W371	A374	N375		3.2, 3.1
	F372	N375			3.5

366-375	E366		A370		2.3
	E367		W371		2.4
	D368	W371	F372		2.6, 2.0
	Q369		E373		2.1
	A370		A374		2.1
	W371	A374	N375		2.9, 2.3
	F372	N375			2.8

366-375	E366		A370		3.2
	E367	A370	W371		3.3, 3.0
	D368	W371	F372		2.9, 2.7
	Q369		E373		2.8
	A370		A374		3.1
	W371		N375		3.1
	F372	N375			3.2

379-393	W379	H382	Y383	G384	2.4, 2.6, 2.1
	A380			K385	2.5
	D381				
	H382	K385	I386		2.8, 2.3
	Y383	I386	F387		2.7, 2.0
	G384		N388		2.2
	K385		E389		2.2
	I386	E389	W390		2.7, 2.1
	F387	W390	K391		2.8, 2.1
	N388		K392		2.2
	E389	K392	L393		2.7, 2.2
	W390	L393			2.6

379-393	W379	A380	D381	H382	3.2, 3.0, 2.8
	A380			K385	3
	D381				
	H382	K385	I386		3.3, 3.1
	Y383	I386	F387		3..0, 2.8
	G384		N388		3
	K385		E389		3
	I386	E389	W390		3.1, 3.0
	F387	W390	K391		3.2, 3.0
	N388		K392		3
	E389		L393		3
	W390	L393			3

379-393	W379	H382	Y383	G384	2.5, 2.7, 2.1
	A380			K385	2.5
	D381				
	H382	K385	I386		2.9, 2.5
	Y383	I386	F387		2.6, 2.2
	G384		N388		2.2
	K385		E389		2.1
	I386	E389	W390		2.6, 2.1
	F387	W390	K391		2.9, 2.1
	N388		K392		2.2
	E389	K392	L393		2.7, 2.3
	W390	L393			2.5

379-393	W379	H382	Y383	G384	3.4, 2.9, 2.8
	A380			K385	3.1
	D381				
	H382				
	Y383	I386	F387		3.0, 2.9
	G384		N388		3
	K385		E389		3
	I386		W390		3
	F387		K391		3.1
	N388		K392		3.2
	E389	K392	L393		3.0, 2.9
	W390	L393			3.1

404-411	P404				2.5,2.0
	Y405				2.8, 2.3
	Q406				2.9,2.1
	W407		W407	L408	2.9, 2.4
	L408		L408	L409	2.6
			L409	A410	
451-459	D451		A410	N411	2.4
	W452	R4	N411	56	2.9, 2.4
	G453	Q456	W457		2.8, 2.1
	E454	W457	L458		2.7, 2.0
	R455	L458	I459		2.8, 2.1

404-411	P404	W407	L408		3.0, 2.9
	Y405		L409		3.2
	Q406		A410		2.9
	W407		N411		3.1
	L408	N411			3.2
451-459	D451		R455		3.2
	W452	R455	Q456		3.4, 3.1
	G453		W457		2.9
	E454		L458		2.9
	R455	L458	I459		3.3, 3.0

404-411	P404	W407	L408		2.4, 2.1
	Y405	L408	L409		2.8, 2.5
	Q406	L409	A410		2.8, 2.2
	W407		N411		2.7
	L408	N411			2.3
451-459	D451		R455		2.6
	W452		Q456		2.5
	G453	Q456	W457		2.8, 2.1
	E454	W457	L458		2.8, 2.0
	R455	L458	I459		2.9, 2.1

404-411	P404		L408		2.9
	Y405	L408	L409		3.2, 3.3
	Q406		A410		3.2
	W407		N411		3.3
	L408	N411			3.1
451-459	D451		R455		3.3
	W452		Q456		3.3
	G453		W457		2.8
	E454		L458		2.7
	R455		I459		2.9

461-463	E460				
	P461				
469-473	V469		Y473		2
478-485	L478	V481	I482		2.6, 2.2
	S479		A383		2.2
	E480		E484		2.2
	V481		G485		2.3
	I482	G485			2.7
509-515	L509	I512	K513		2.7, 2.0
	E510		R514		2.3
	D511				
	I512	A515			2.2

461-463	E460				
	P461				
469-473	N478				
	V469				
478-485	L478	V481	I482		3.1, 3.0
	S479		A483		3
	E480		E484		3
	V481		G485		3
	I482	G485			3.1
509-515	L509	I512	K513		3.2, 2.8
	E510		R514		3
	D511				
	I512	A515			2.8

461-463	E460				
	P461				
469-473	N478				
	V469				
478-485	L478	V481	I482		2.6, 2.2
	S479		A483		2.1
	E480		E484		2.1
	V481		G485		2.2
	I482	G485			2.6
509-515	L509	I512	K513		2.7, 2.0
	E510		R514		2.3
	D511				
	I512	A515			2.3

461-463	E460				
	P461				
469-473	V469		Y473		2.9
478-485	L478	V481	I482		3.1, 3.2
	S479		A483		2.9
	E480		E484		3.1
	V481		G485		2.9
509-515	L509	I512	K513		3.2, 3.0
	E510		R514		3
	D511				
	I512	A515			2.9

hydrogen bonding = i + 3 (3_{10} helix)
hydrogen bonding = i + 4 (α-helix)
hydrogen bonding = i + 5 (π-helix)
hydrogen bonding lost in this region relative to other structures

Table S5. Interatomic Distances for sMMOH:MMOB

Complex	sMMOH^{ox}:MMOB				sMMOH^{red}:MMOB	
Type	Form 1 (6VK5)		Form 2 (6VK8)		(6VK4)	
	Protomer 1	Protomer 2	Protomer 1	Protomer 2	Protomer 1	Protomer 2
Resolution	1.86 Å	1.86 Å	2.03 Å	2.03 Å	2.35 Å	2.35 Å
Fe1-Fe2	3.5	3.5	3.4	3.5	3.5	3.2
Fe1-E114 OE1	2.1	1.9	2.0	1.9	1.9	2.0
Fe1-E144 OE1	2.1	2	2.1	2.1	2.1	2.0
Fe1-E243 OE2	3.7	3.8	3.9	3.9	3.4	2.2
Fe1-H147 ND1	2.3	2.2	2.2	2.2	2.1	2.3
Fe1-HOH 1	2.2	2.0	2.2	2.2	2.1	2.1
Fe1-HOH 2[a]	2.0	2.0	2.0	1.9	1.9	N/A
Fe1-BEZ/SIN O1	2.1	2.1	1.9	1.9	2.0	1.9
Fe2-E209 OE2	2.1	2.2	2.3	2.1	2.1	2.1
Fe2-E243 OE2	3.2	3.4	3.5	3.6	3.3	2.2
Fe2-E243 OE1	2.3	2.2	2.2	2.2	2.0	2.1
Fe2-E144 OE2	2.2	2.1	2.3	2.2	2.0	2
Fe2-H246 ND1	2.3	2.2	2.3	2.2	2.2	2.1
Fe2-BEZ /SIN O2	2.2	2.2	2.5	2.3	2.1	2.2
Fe2-HOH 2[a]	2.0	1.9	1.8	2.0	1.9	N/A

[a]bridging

Comparison of Structures from Data for Crystals at 100K/Synchrotron versus Room Temperature/XFEL. An alignment of the room temperature RT-XFEL[6] and cryogenic (100 K) synchrotron *Mt* sMMOH:MMOB structures at comparable resolution (cf. 1.95 Å – 6YD0, 1.86Å – 6VK5) shows that structural changes are concentrated in the α-subunit of sMMOH. A comparison of RMSD values is shown in Table S6 and Figure S2. For the sMMOH^{ox}:MMOB structures, it was found that the β- and γ-subunits of sMMOH align well (RMSD = 0.33 Å for β and 0.21 for γ). In contrast, the α-subunits align slightly less well (RMSD = 0.71 Å). This difference is mainly due to the structural changes caused by exogenous molecule binding in the active site of the cryogenic structures. These findings indicate that there is little difference between structures determined using diffraction from crystals at room temperature versus those at 100 K. This observation is also borne out by the comparison between the original room temperature structure of sMMOH (1MHY, 2.0 Å resolution)[4] and the 1.52 Å cryo structure of MMOH from this study (RMSD = 0.26 Å for α; 0.19 Å for β and 0.19 for γ).

Table S6. Structural Alignment Average RMSD Values (Å)[a]

sMMOH Subunits	Form 1 vs. Form 2	Form 1 reduced vs. Form 1	Form1 vs. XFEL H^{ox}B[b]	sMMOH^{ox} vs. 1MHY	sMMOH^{ox} vs. Form1[b]	sMMOH^{ox} vs. sMMOH^{red}
α1-α1	0.159	0.190	0.703	0.265	0.857	0.474
α1-α2	0.182	0.185	0.707	NA[b]	0.883	N/A[b]
β1-β1	0.129	0.167	0.342	0.195	0.277	0.188
β1-β2	0.147	0.160	0.33	NA[b]	0.267	N/A[b]
γ1-γ1	0.112	0.160	0.22	0.191	0.206	0.155
γ1-γ2	0.13	0.144	0.208	NA[b]	0.192	N/A[b]

[a]Form 1 = sMMOH^{ox}:MMOB (6VK5); Form 2 = sMMOH^{ox}:MMOB (6VK8); Form 1 reduced = sMMOH^{red}:MMOB (6VK4); XFEL H^{ox}B = sMMOH^{ox}:MMOB (6YD0); XFEL H^{red}B = sMMOH^{red}:MMOB (6YDI); sMMOH^{ox} (6VK6); sMMOH^{red} (6VK7); 1MHY is previously submitted *Mt* sMMOH^{ox} with data recorded at 20 °C resolution = 2 Å.[4]

[b]The crystals of sMMOH^{ox} ,sMMOH^{red}, and XFEL H^{ox}B have 2-fold crystallographic symmetry, unlike the crystals of the other enzyme forms in this table which have both αβγ protomers in the asymmetric unit. Consequently, α, β, and γ subunits of sMMOH$^{ox/red}$ and XFEL H^{ox}B are compared with both α, β, and γ subunits in the asymmetric units of the other crystals.

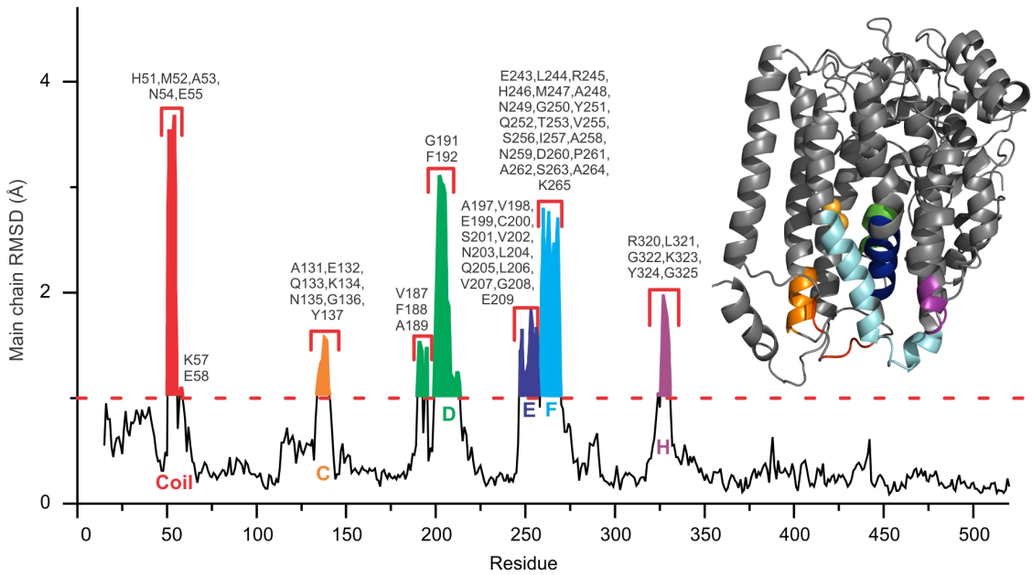

Figure S2. Main chain Cα RMSD comparison of the structures of the α-subunits of Form 1 sMMOH^{ox}:MMOB (6VK5) with RT-XFEL sMMOH^{ox}:MMOB (6YD0). These structural changes occur as a result of binding of an exogenous molecule (benzoate) in the active site of sMMOH. The majority of the changes occur in three out of four helices of the four-helix bundle housing the diiron cluster (C, E and F) and Helix D that forms the outer border of the active site cavity. This reorganization in turn rearranges an extended coil region in contact with Helices C, E and F and Helix H that is in contact with Helix E. *Inset*: Cartoon of the α-subunit with color coding to showing the regions that change in structure. The diiron cluster is shown as gold spheres.

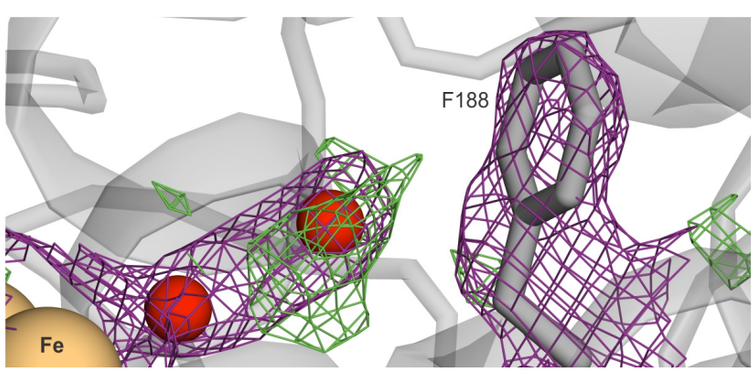

Figure S3. Unassigned electron density in the active site of *Mc* sMMOH^{ox} (PDB:4GAM, Chain A). The 2Fo-Fc map (1.2 σ) is represented as purple isomesh and the Fo-Fc map (+3 σ) is represented as green isomesh. The green Fo-Fc isomesh indicates that the two waters (red spheres) modeled into the active site do not account for all of the experimental density. Three of the four subunits in the asymmetric unit of the 4GAM model have positive sigma density altering the position of F188 and enlarging the connection between Cavities 2 and 1.

Table S7. The W308 Tunnel Residues are Conserved Amongst 15 Small Hydrocarbon Oxidizing Strains[a]

	Sub[b]	110	188	192	212	213	215	216	217	219	222	223	282	286	290	299	301	304	305	308	309
Methylosinus trichosporium OB3b	CH_4	L	F	F	F	T	P	L	I	A	E	W	F	L	F	E	W	T	W	W	V
Methylococcus capsulatus Bath	CH_4	L	F	F	F	T	P	L	I	A	E	W	F	L	F	E	W	T	W	W	V
Sphingobium sp. SCG-1	CH_4	L	F	F	F	T	P	L	I	A	E	W	F	L	F	E	W	T	W	W	V
Methylospira mobilis	CH_4	L	F	F	F	T	P	L	I	A	E	W	F	L	F	E	W	T	W	W	V
Methylomicrobium japanense	CH_4	L	F	F	F	T	P	L	I	A	E	W	F	L	F	E	W	T	W	W	V
Methylomonas methanica	CH_4	L	F	F	F	T	P	L	I	A	E	W	F	L	F	E	W	T	W	W	V
Crenothrix polyspora	CH_4	L	F	F	F	T	P	L	I	A	E	W	F	L	F	E	W	T	W	W	V
Methylovulum miyakonense HT12	CH_4	L	F	F	F	T	P	L	I	A	E	W	F	L	F	E	W	T	W	W	V
Betaproteobacteria bacterium	CH_4	L	F	F	F	T	P	L	I	G	E	W	F	L	F	E	W	T	W	W	V
Rhodospirillaceae bacterium	CH_4	L	L	F	F	T	P	L	I	A	E	W	I	V	L	E	W	T	W	W	V
Mycolicibacterium elephantis	CH_4	L	A	F	F	T	P	L	V	A	E	W	L	V	F	E	W	T	W	W	V
Mycolicibacterium rhodesiae	CH_4	L	F	F	F	T	P	L	I	A	E	W	A	V	F	E	W	V	W	W	V
Mycobacterium chubuense NBB4	C_3H_8	L	F	F	F	T	P	L	I	A	E	W	A	V	F	E	W	V	W	W	V
Thauera butanivorans	CH_4	L	F	F	F	T	P	L	I	S	E	W	L	V	L	E	W	S	W	W	V
Brachymonas petroleovorans	C_4H_{10}	L	F	F	F	T	P	L	I	A	E	W	L	V	L	D	W	M	W	W	V

[a]BLAST alignment of α-subunit W308-tunnel residues, *Methylosinus trichosporium* OB3b numbering. NCBI GenBank sequence ID: *Methylosinus trichosporium* OB3b - CAA39068.2, *Methylococcus capsulatus Bath* - WP_010960482.1, *Sphingobium* sp. SCG-1 - WP_104955546.1, *Methylospira mobilis* - WP_153249048.1, *Methylomicrobium japanense* - BAE86875.1, *Methylomonas methanica* - WP_013818321.1, *Crenothrix polyspora* - WP_087143657.1, *Methylovulum miyakonense* HT12 - BAJ17645.1, Betaproteobacteria bacterium - PKO92487.1, *Rhodospirillaceae* bacterium - PCJ58204.1, *Mycolicibacterium elephantis* - WP_046753692.1, *Mycolicibacterium rhodesiae* - WP_014211362.1, *Mycobacterium chubuense* NBB4 - ACZ56334.1, *Thauera butanivorans* - WP_068635403.1, *Brachymonas petroleovorans* - AAR98534.1.

[b]Substrate for the diiron monooxygenase

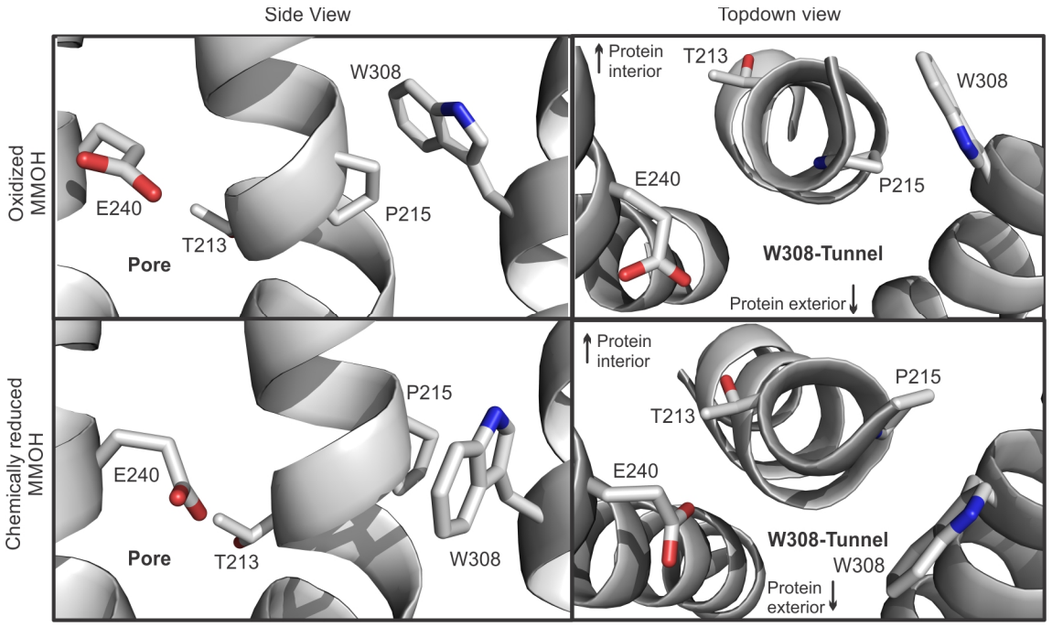

Figure S4. Effect of diiron cluster reduction on the Pore (left) and the W308-Tunnel (right). Reduction of sMMOH causes the Pore to partially close and opens the entrance into the W308-Tunnel. However, a bottleneck remains at sMMOH F282 and F212 that is not relieved until a complex is formed with MMOB (see Figures 8 and 13 in the main text). The Pore is fully closed in the sMMOH:MMOB complex (see Figure 6). $sMMOH^{ox}$ = PDB:6KV6; $sMMOH^{red}$ = PDB:6VK7.

Table S8. Steady State O_2 Uptake in the Reconstituted sMMO System with MMOB Variants[a]

MMOB Variant	Variant Alone % Activity	Variant 1:1 with MMOB % Activity	Variant 5:1 with MMOB % Activity
None (MMOH alone)	0	N/A	N/A
WT-MMOB	100	100	100
V39F	< 0.1	100	86
V39R	< 0.1	84	42
V41E[b]	< 0.1	100	100
V41F[b]	< 0.1	100	100
V41R	< 0.1	53	4

[a]Conditions: 0.2 μM sMMOH (0.4 μM active sites), 0.4 μM MMOB, 0.4 μM or 2.0 μM MMOB variant when present 1.2 μM MMOR, 200 μM CH_4, 250 μM O_2, 400 μM NADH, 25 mM MOPS pH 7.5, 23 °C

[b]Steady state data alone do not demonstrate binding for these variants. However, a perturbation in the EPR spectrum of reduced sMMOH shows that these variants do form a complex (see below).

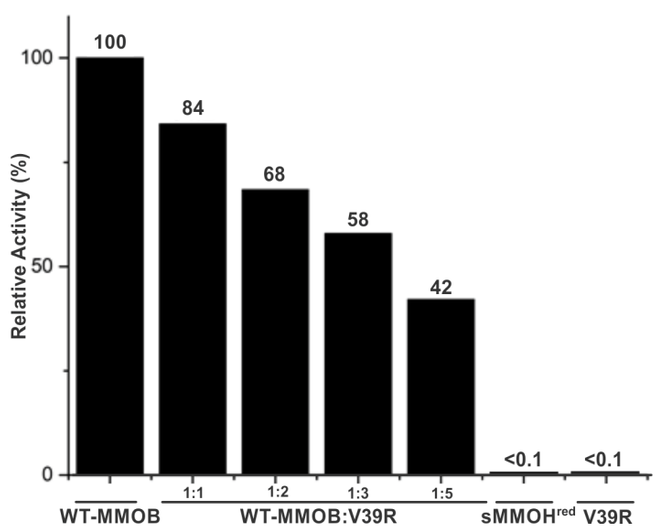

Figure S5. Competition between WT-MMOB and V39R-MMOB during steady state turnover. *Mt* sMMOH is present at the same concentration in all experiments. When WT-MMOB or V39R-MMOB was added alone, it was present at the same concentration as MMOH (active sites). For experiments in which WT-MMOB and V39R are added together in the ratios shown, WT-MMOB is present at the same concentration as sMMOH (active sites). Other conditions for the experiment are given in Experimental Procedures.

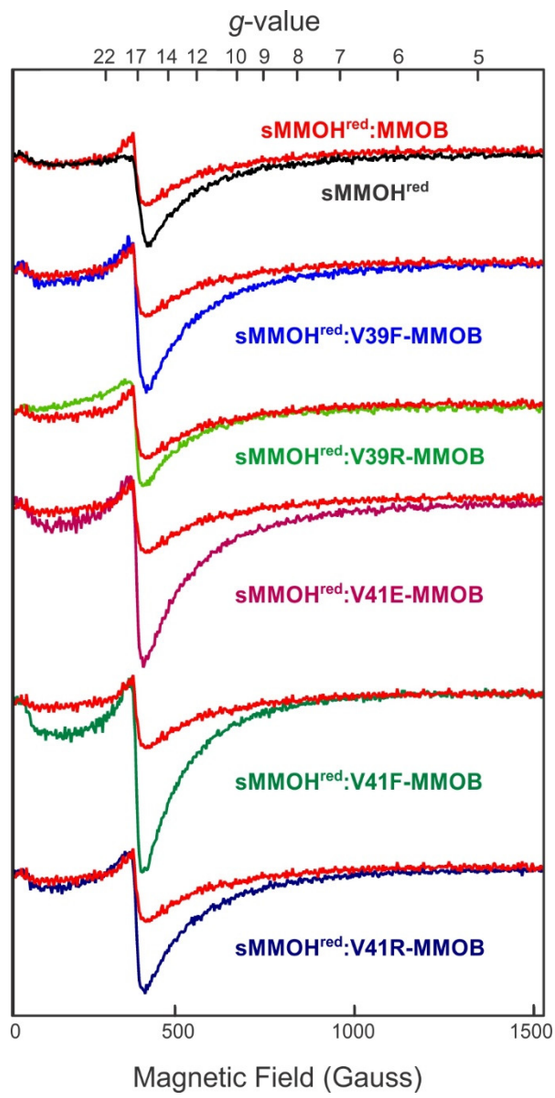

Figure S6. Parallel mode EPR spectra of sMMOH^{red} with MMOB and MMOB variants. sMMOH^{red} exhibits a characteristic EPR spectrum at g = 16 due to ferromagnetic coupling of the two high-spin Fe(II) ions of the diiron cluster.[7, 8] The resulting integer spin system gives an enhanced EPR signal when recorded with the microwave field aligned parallel with the magnetic field.[9] The signal is perturbed when MMOB is present due to the formation of a protein-protein complex (compare the black and red spectra in the top trace). Each of the MMOB variants used in this study gives a similar perturbation, albeit with distinct intensities, showing that each forms a complex with MMOH^{red} (red trace from sMMOH:MMOB show for comparison in each case). Moreover, each perturbs the diiron cluster environment slightly differently. Conditions: sMMOH^{red}, 300 μM (active sites); MMOB (or variant), 300 μM, 25 mM MOPS, pH 7.5. EPR conditions: frequency, 9.400 GHz; time constant, 2.56 ms; microwave power, 2 mW, temperature, 2.0 K, cavity tuned for parallel mode detection.

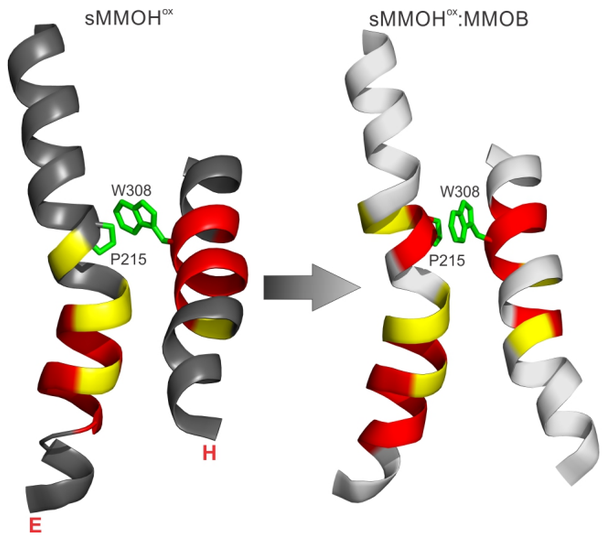

Figure S7. The W308-Tunnel molecular gate. sMMOH amino acids P215 (Helix E) and W308 (Helix H) shift dramatically upon formation of the MMOB complex, acting as a molecular gate. The gate movement is possible because of the π-helices (red) and sections of the helix that do not form intra-main chain hydrogen bonds (yellow). As a result the helices are more flexible allowing the molecular gate to open and close. sMMOH^{ox} = PDB:6VK6; sMMOH^{ox}:MMOB = PDB:6YD0.

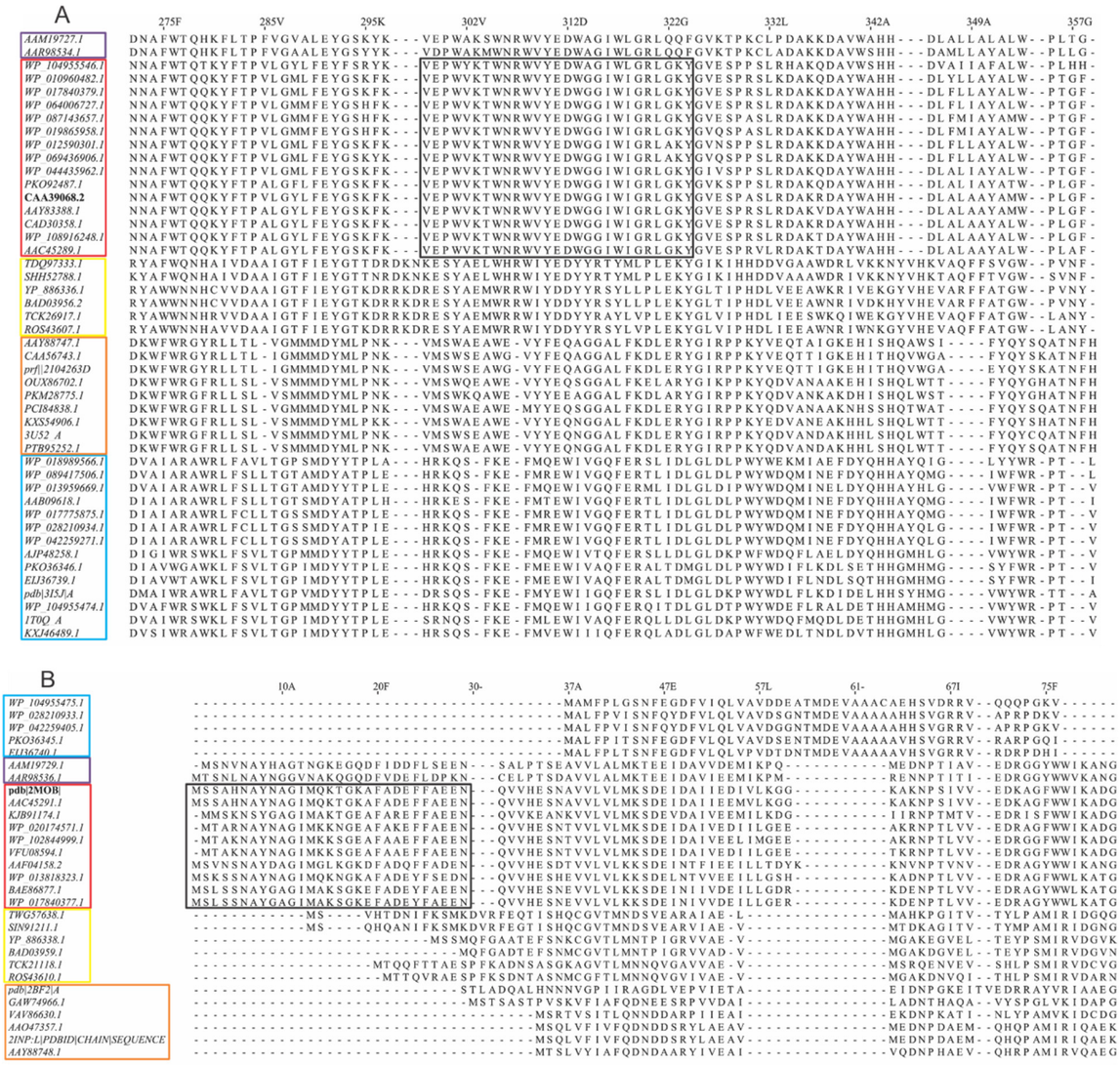

Figure S8. Sequence alignments of key regions of hydroxylase and regulatory proteins. Portions of the α-subunit of the hydroxylase components (panel A) and the regulatory protein components (panel B) of the bacterial multicomponent monooxygenase family are illustrated. Enzyme sub-families are identified by colored boxes; methane monooxygenase – red, butane monooxygenase – purple, propane monooxygenase – yellow, phenol hydroxylase – orange, toluene monooxygenase – cyan. The unique extended N-terminal tail of the regulatory component and the tryptophan-rich Helix H of the α-subunit in sMMOH have been highlighted by black boxes.

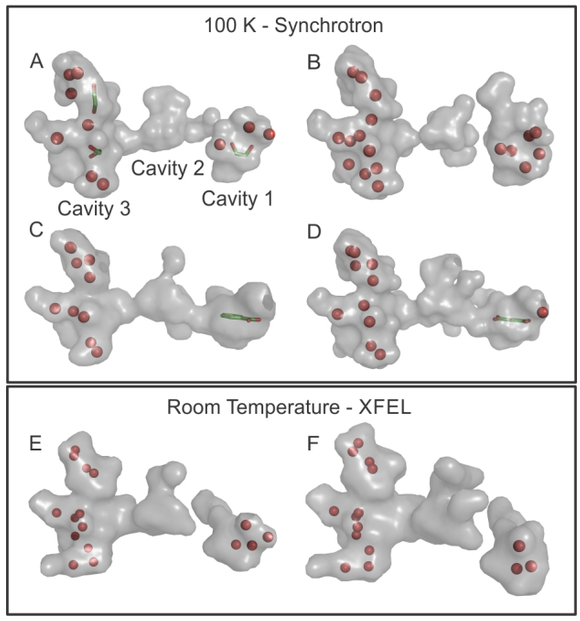

Figure S9. Exogenous molecules bound inside the cavities. The chain of *Mt* sMMOH internal cavities is represented as transparent gray surface. Water molecules are represented as red spheres. Alternative substrate molecules are shown as sticks where green is carbon and red is oxygen. A.) *Mt* sMMOH^{ox} (6VK6), B.) *Mt* sMMOH^{red} (6VK7), C.) *Mt* sMMOH^{ox}:MMOB, Form 1, protomer 1 (6VK5), D.) *Mt* sMMOH^{ox}:MMOB, Form 2, protomer 1 (6VK8), E.) RT-XFEL *Mt* sMMOH^{ox}:MMOB (6YD0),[6] F.) RT-XFEL *Mt* sMMOH^{red}:MMOB (6YDI).[6]

Supplemental References

[1] Groce, S. L., Miller-Rodeberg, M. A., and Lipscomb, J. D. (2004) Single-turnover kinetics of homoprotocatechuate 2,3-dioxygenase, *Biochemistry 43*, 15141-15153.

[2] Whittaker, J. W., and Lipscomb, J. D. (1984) Transition state analogs for protocatechuate 3,4-dioxygenase. Spectroscopic and kinetic studies of the binding reactions of ketonized substrate analogs, *J. Biol. Chem. 259*, 4476-4486.

[3] Rosenzweig, A. C., Frederick, C. A., Lippard, S. J., and Nordlund, P. (1993) Crystal structure of a bacterial non-haem iron hydroxylase that catalyses the biological oxidation of methane, *Nature 366*, 537-543.

[4] Elango, N., Radhakrishnan, R., Froland, W. A., Wallar, B. J., Earhart, C. A., Lipscomb, J. D., and Ohlendorf, D. H. (1997) Crystal structure of the hydroxylase component of methane monooxygenase from *Methylosinus trichosporium* OB3b, *Protein Sci. 6*, 556-568.

[5] Sazinsky, M. H., and Lippard, S. J. (2005) Product bound structures of the soluble methane monooxygenase hydroxylase from *Methylococcus capsulatus* (Bath): Protein motion in the a-subunit, *J. Am. Chem. Soc. 127*, 5814-5825.

[6] Srinivas, V., Banerjee, R., Lebrette, H., Jones, J. C., Aurelius, O., Kim, I.-S., Pham, C. C., Gul, S., Sutherlin, K. D., Bhowmick, A., John, J., Bozkurt, E., Fransson, T., Aller, P., Butryn, A., Bogacz, I., Simon, P., Keable, S., Britz, A., Tono, K., Kim, K. S., Park, S.-Y., Lee, S. J., Park, J., Alonso-Mori, R., Fuller, F. D., Batyuk, A., Brewster, A. S., Bergmann, U., Sauter, N. K., Orville, A. M., Yachandra, V. K., Yano, J., Lipscomb, J. D., Kern, J., and Högbom, M. (2020) High resolution XFEL structure of the soluble methane monooxygenase hydroxylase complex with its regulatory component at ambient temperature in two oxidation states, *J. Am. Chem. Soc.*, *https://doi.org/10.1021/jacs.0c05613*

[7] Fox, B. G., Froland, W. A., Dege, J. E., and Lipscomb, J. D. (1989) Methane monooxygenase from *Methylosinus trichosporium* OB3b. Purification and properties of a three-component system with high specific activity from a type II methanotroph, *J. Biol. Chem. 264*, 10023-10033.

[8] Froland, W. A., Andersson, K. K., Lee, S.-K., Liu, Y., and Lipscomb, J. D. (1992) Methane monooxygenase component B and reductase alter the regioselectivity of the hydroxylase component-catalyzed reactions. A novel role for protein-protein interactions in an oxygenase mechanism, *J. Biol. Chem. 267*, 17588-17597.

[9] Hendrich, M. P., Münck, E., Fox, B. G., and Lipscomb, J. D. (1990) Integer-spin EPR studies of the fully reduced methane monooxygenase hydroxylase component, *J. Am. Chem. Soc. 112*, 5861-5865.